Where applicable, the authors confirm that the experiments described here conform with The Physiological Society ethical requirements.

C5 and PC54

Sensitised renal sympathoexcitatory response to spinal vasopressin and glutamate infusion in Wistar rats fed a high Na^+ diet

B.L. Houghton and E.J. Johns

Physiology, University College Cork, Cork, Ireland

Vasopressinergic neurons which project from the paraventricular nucleus to the spinal cord (Hallbeck & Blomqvist, 1999) facilitate renal (Yang & Coote, 2006) and lumbar (Antunes *et al*. 2006) sympathoexcitation (SNA) by the release of AVP and glutamate. Increased lumbar SNA by acute salt loading is partially mediated by spinal V1 receptor activation (Antunes et al. 2006). Our lab has shown that Wistar rats fed a high Na^+ (HNa^+) diet from weaning to adulthood exhibited an enhanced blood pressure (BP) and renal sympathoexcitatory (RSNA) response to lateral intracerebroventricle infusion of angiotensin III (Houghton & Johns, 2007). The pressor response was attenuated by peripheral V_1 blockade, but the RSNA response remained, which suggested a role for spinal V1 receptor activation. It was hypothesised that the RSNA response to intrathecal (IT) infusion of vasopressin or glutamate would be augmented in HNa^+ rats.

Four week old male Wistar rats were fed a normal Na^+ (0.3%, NNa^+) or high Na^+ (3.0%) diet for six weeks and anaesthetised by a 1 ml chloralose/urethane (16.5/250mg/ml) I.P. injection. Cannulae were inserted into the right femoral artery (BP measurement) and vein (saline/anaesthetic infusions). An intrathecal (IT) cannula filled with artificial cerebrospinal fluid (aCSF, pH 7.4) was inserted at vertebra L3 and the tip placed at T13. The left kidney was exposed and recording electrodes were sealed onto a renal nerve. The RSNA response to IT AVP (1, 5, 10, 20μM; 10 μL/2min; NNa^+ = 7, HNa^+ = 5) or IT glutamate (10, 20, 50, 100mM, 10 μL/2min; NNa^+ = 6, HNa^+ = 5) was recorded for 15 min. RSNA was averaged over a 2-min period during baseline measurements and over 60 seconds at the peak RSNA response. Background RSNA noise recorded after the experiment was terminated was subtracted from the original values. Peak RSNA was calculated as percentage of baseline values prior to each IT infusion. Means ± S.E.M. were compared by ANOVA.

Baseline RSNA (μV/s) was similar between groups (NNa^+:13±2 vs HNa^+: 9±2). The peak rise in RSNA after IT AVP infusion was greater in HNa^+ at 1μM* (NNa^+: 100±2% vs HNa^+: 108±2.0%) and 5μM* (NNa^+: 103 ± 1% vs HNa^+: 110±2%). A sensitised RSNA response to IT glutamate infusion was also observed in HNa+ after 10mM** (NNa^+: 98 ± 1% vs HNa^+: 117±5%), 20mM* (NNa^+: 105±4% vs HNa^+: 130±12%), 50mM** (NNa^+: 109±2% vs HNa^+:147±6%) and 100mM** (NNa^+: 126±8% vs HNa^+: 178±26%). All comparisons reached significance of *P<0.05 or **P<0.01.

These results show that HNa^+ intake sensitises the RSNA response to IT AVP and glutamate infusion. This suggests that spinal AVP- and glutamate-mediated RSNA may be enhanced and could contribute to the development of hypertension due to long term high dietary Na^+ intake.

Antunes VR, Yao ST, Pickering AE, Murphy D & Paton JFR (2006). *J Physiol* 576, 569-583.

Hallbeck M & Blomqvist A (1999). *J Comp Neurol* 411, 201-211.

Houghton BL & Johns EJ (2007). Impact of sodium intake on the blood pressure and renal sympathetic nerve activity during intracerebroventricle infusion of angiotensin III in anaesthetised Wistar Rats. Royal Academy of Medicine in Ireland (RAMI) Annual Meeting. Oral communication.

Yang Z & Coote JH (2006). *Exp Physiol* 91, 791-797.

Funding: Health Research Board (RP/2004/17).

Where applicable, the authors confirm that the experiments described here conform with The Physiological Society ethical requirements.

C6 and PC55

Amygdala projecting solitary tract nucleus neurons receive both direct and indirect cranial visceral afferent connections

S. McDougall and M. Andresen

Physiol/Pharmacol, OHSU, Portland, OR, USA

The solitary tract nucleus (NTS) is the central site of afferent termination of the IXth and Xth cranial nerves. Information arrives in the NTS via the solitary tract and is subsequently broadcast to other brain regions including the amygdala. Little is known about the organization and processing of such information by forebrain projecting NTS neurons that likely contribute to complex behaviors. We aimed to determine if cranial visceral afferents contact amygdala projecting NTS neurons directly or indirectly using retrograde tracing and electrophysiological techniques. Sprague-Dawley rats were anaesthetized (ketamine 60 mg/kg, xylazene 6 mg/kg, acepromazine 1 mg/kg; i.p.) for a stereotaxic procedure in which rhodamine beads (100 nl) were injected into the central nucleus of the amygdala. Anaesthesia level was monitored by foot pinch and corneal reflex tests throughout surgery. After 2 – 4 weeks animals were deeply anesthetized (5% isoflurane by inhalation) and horizontal brainstem slices (250 μm) containing both the NTS and solitary tract were taken. Retrogradely labeled cell bodies were found distributed throughout the caudal NTS and were targeted for whole cell recordings. Shocks to the solitary tract evoked glutamate mediated EPSCs in the labeled neurons. Each neuron was characterized by detailed stimulus-recruitment curves – where the latency, magnitude and kinetics of evoked postsynaptic currents were related to shock intensity. Some amygdala projecting NTS neurons exhibited constant latency solitary tract-evoked EPSCs that rarely failed and exhibited frequency dependent depression to a train of shocks. These characteristics are consistent with direct afferent contacts (via the solitary tract) onto labeled NTS neurons and similar to most cells within the NTS if surveyed randomly. The majority of labeled neurons exhibited multiple glutamatergic EPSCs and GABAergic IPSCs with highly variable latencies and frequent failures – findings consistent with polysynaptic pathways from

to spikes revealed that they were triggered by 3 or more distinct unitary EPSPs in 19/39 MVC-type ganglion cells. Small EPSPs very rarely summed to reach threshold. Observations on EPSPs after blocking spikes with hyperpolarizing current confirmed these conclusions. Another new finding was the common occurrence of intermediate-sized (10-20 mV) unitary EPSPs in 16/39 MVC-type cells. These were not far below threshold (estimated as ~18 mV above resting potential).
Our data thus confirm that 'strong' EPSPs essentially determine spike activity in putative vasomotor ganglion cells, leaving little room for synaptic integration. Convergence of strong preganglionic inputs is greater than previously suspected, however, and the existence of 'intermediate'-sized EPSPs provides the potential to enhance ganglionic throughput by a modest change in cell threshold.

1. Jänig W (1988). Annu Rev Physiol 50, 525-539.

2. McLachlan EM, Davies PJ, Habler HJ & Jamieson J (1997). J Physiol 501, 165-181.

3. McLachlan EM, Habler HJ, Jamieson J & Davies PJ (1998). J Physiol 511, 461-478.

This work supported by a grant from NHMRC. W.J. received an Allen and Maria Myers Visting Fellowship to work at the Howard Florey Institute.

Where applicable, the authors confirm that the experiments described here conform with The Physiological Society ethical requirements.

C9 and PC58

Ovariectomy modifies sympathetic neuropeptide Y control of hindlimb vasculature in female Sprague-Dawley rats

D.N. Jackson[1], J. Shoemaker[2] and E. Noble[2]

[1]Medical Biophysics, The University of Western Ontario/Schulich School of Medicine & Dentistry, London, ON, Canada and [2]Kinesiology, The University of Western Ontario, London, ON, Canada

Neuropeptide Y (NPY) is a peptide transmitter released from sympathetic neurons, promoting potent and prolonged vasoconstriction. We recently reported that male (1), but not female, rats exhibited baseline endogenous NPY Y1-receptor (Y1R) modulation of hindlimb vasculature (2). The lack of Y1R control in females was evident despite Y1R expression and NPY in the hindlimb. Subsequently, we observed that female rats limit NPY bioavailability via activation of inhibitory NPY Y2-receptors (Y2R), greater skeletal muscle Y2R expression and NPY metabolism via augmented peptidase activity (3). In this investigation we sought to determine the underlying mechanism(s) governing the sexual dimorphism in NPY control of skeletal muscle vasculature. We tested the hypothesis that estrogen minimizes NPY bioavailability and/or Y1R vasomotor control in skeletal muscle. Thus, we examined whether ovariectomy would expose an important contribution of endogenous Y1R activation to baseline blood flow in female rats as a result of 1) increased skeletal muscle Y1R expression, 2) increased skeletal muscle NPY, and 3) decreased peptidase activity. We further assessed whether estrogen replacement would reverse the impact of ovariectomy on cellular and functional vascular responses. In terminal experiments, animals were anaesthetized by intraperitoneal injection of α-chloralose (80 mg/kg) and urethane (500 mg/kg). Animals were killed by anaesthetic overdose. Recovery surgeries (i.e. ovariectomy and hormone pellet insertion) were carried out under pentobarbital anaesthesia.
In ovariectomized rats treated with estradiol placebo (OVX, n=7), localized hindlimb arterial infusion of the Y1R antagonist BIBP3226 (100 μg/kg) increased blood flow (Δ from baseline = 270.2$\pm$74 μl/min) and vascular conductance (Δ from baseline = 2.96$\pm$0.95 μl/min/mmHg) (mean $\pm$ SEM, one-way ANOVA, $P<0.05$). In contrast, Y1R blockade had no vascular effect on the control group (CTRL, n=5) or on ovariectomized rats treated with 17β-estradiol (OVX+E2, n=6). The OVX group had augmented Y1R expression in white vastus muscle (WV) (one-way ANOVA, $P<0.05$, Western blot, n=8 per group) compared to the CTRL group; this effect of ovariectomy was not apparent in the OVX+E2 group (expressed in arbitrary units: CTRL = 87.6 vs. OVX = 107.4 vs. OVX+E2 = 78.9). Y1R expression was unchanged by any intervention in red vastus muscle (RV). In WV and RV, NPY concentration was elevated in OVX compared to CTRL and OVX+E2 (WV CTRL = 12$\pm$1.5 pg/μg vs. OVX = 21$\pm$2.4 pg/μg vs. OVX+E2 = 10$\pm$1 pg/μg; RV CTRL = 24$\pm$3.7 vs. OVX = 61$\pm$1.3 pg/μg vs. OVX+E2 = 31$\pm$4.7 pg/μg)(one-way ANOVA, $P<0.05$,ELISA, n=8 per group). Peptidase activity was unchanged among groups. Our data indicate that estrogen blunts Y1R activation in the hindlimb of baseline female rats due to an impact on Y1R expression and NPY bioavailability.

Jackson DN, Noble EG & Shoemaker JK (2004). Am J Physiol Regul Integr Comp Physiol 287, R228-R233.

Jackson DN, Milne KJ, Noble EG & Shoemaker JK (2005). J Physiol 562, 285-294.

Jackson DN, Milne KJ, Noble EG & Shoemaker JK (2005). J Physiol 568, 573-581.

Supported by the Canadian Institutes of Health Research.

Where applicable, the authors confirm that the experiments described here conform with The Physiological Society ethical requirements.

C10 and PC59

Endothelial overexpression of NADPH oxidase Nox4 in mice *in vivo* enhances vasorelaxation and lowers blood pressure

R. Ray[1], M. Zhang[1], A. Ouattara[2], A. Cave[1], A. Brewer[1] and A. Shah[1]

[1]Department of Cardiology, James Black Centre, 125 Coldharbour Lane, King's College London, London, UK and [2]Département d'Anesthésie-Réanimation chirurgicale, Groupe Hospitalier Pitié-Salpêtrière, 47-83 boulevard de l'Hôpital, Paris, France

Oxidative stress is implicated in the genesis of cardiovascular diseases through the inactivation of nitric oxide and modulation of redox-sensitive signalling pathways. A family of NADPH oxidases (Noxs) form an important source of reactive oxygen species (ROS) within the vessel wall, with the Nox2 and Nox4

isoforms being the major contributors to endothelial ROS. The involvement of Nox2 in endothelial dysfunction is well established, but the role of Nox4 remains uncertain with recent evidence indicating that it has distinct mechanisms of regulation to Nox2. The aim of the present study was to investigate the *in vivo* role of Nox4 in the endothelium.

Transgenic mice (Tg) were generated with endothelial-targeted overexpression of Nox4 using a Tie2 promoter construct, and were backcrossed into a C57Bl6/j background. Tg mice had 2-fold greater Nox4 mRNA expression and 3-fold greater Nox4 protein in coronary microvascular endothelial cells (CMEC) compared with wild-type littermates (WT)(n=4; $p<0.05$). Tg CMEC had increased NADPH-dependent superoxide production (237.6±2.7 *vs*. 186.5±7.1 integrated RLU; n=3, $p<0.01$) and increased hydrogen peroxide generation (homovanillic acid assay) compared to WT (7.60±0.70 *vs*. 3.22±0.42 μM $H_2O_2/10^5$ cells; n=3, $p<0.01$). No changes were noted in expression of p22*phox*, SOD1-3 or catalase mRNA. *In vivo* systolic and diastolic blood pressure measured by telemetry was significantly lower in TG mice compared to WT (systolic 117.4±1.9 *vs*. 125.5±2.1 mmHg and diastolic 90.1±2.0 *vs*. 98.1±2.1 mmHg; n=5, $p<0.05$). Isolated preconstricted aortic rings from TG mice revealed enhanced acetylcholine-induced vasorelaxation compared to WT (-log EC_{50} 7.76±0.07 *vs*. 7.20±0.05; n=12, $p<0.001$), a difference that was abolished by catalase (1500 U/ml). Similarly, coronary microvascular resistance in isolated Langendorff-perfused hearts was reduced to a greater extent by acetylcholine in TG than WT (-log EC_{50} 5.59 ± 0.27 *vs*.4.80 ± 0.48; n=5, $p<0.05$), an effect also abolished by catalase (1500 U/ml). Chronic 7-day administration of the SOD and catalase-mimetic, EUK-8, *in vivo* abolished the difference in blood pressure between TG and WT (Difference 11.7±1.6 mmHg pre- *vs*. 1.6±4.3 mmHg post-EUK-8).

Taken together, these results indicate that overexpression of Nox4 within the endothelium has unforeseen beneficial effects on both vasomotor tone and blood pressure, probably through generation of hydrogen peroxide. These results suggest that endothelial Nox4 and Nox2 have distinct and contrasting functions *in vivo* .

Supported by the British Heart Foundation.

Where applicable, the authors confirm that the experiments described here conform with The Physiological Society ethical requirements.

C11 and PC60

Patterns of respiratory activation for intercostal muscles in the rat

A. de Almeida and P.A. Kirkwood

Sobell Dept Motor Neuroscience & Movement Disorders, UCL Institute of Neurology, London, UK

Cats, dogs and humans show a consistent pattern of intercostal muscle discharges in their dorsal regions, the external layer being inspiratory, the internal layer expiratory (De Troyer et al. 2005). Here we report that the pattern in the rat is different.

Intercostal spaces T6-T10 were studied in vagotomised rats, stimulated with CO_2 to give a strong respiratory drive. Intercostal nerve discharges were recorded in anaesthetized or decerebrate rats, under neuromuscular blockade, as were intracellular recordings from motoneurones with axons in intercostal nerves of T8 or T9. EMG recordings were made from proximal parts of spaces T6-T10 in spontaneously breathing anaesthetized animals.

Anaesthetics: ketamine/xylazine, induction I.P., 100mg/kg, 10mg/kg respectively, maintenance I.V., as required, same ratio; urethane, induction 1.4 g/kg I.P., maintenance 0.2 g/kg I.P. if needed; alpha-chloralose, induction and surgery under halothane, titrated to alpha-chloralose I.V. up to 80 mg/kg for recordings. Decerebration: induction and surgery under halothane or ketamine/xylazine (as above), brain removed rostral to colliculi following other surgery. Neuromuscular blockade: pancuronium bromide I.V., initially 2.5 mg/kg, then 1.7 mg/kg.hr (adequate anaesthesia assured by stability of blood pressure, heart rate and pattern of respiratory discharges following noxious stimuli).

Under ketamine/xylazine or urethane, expiratory discharges were seen only in relatively lightly anaesthetized animals (cf. Saywell et al. 2007) and were weak or intermittent. Only under alpha-chloralose or decerebration were these discharges strong and regular. In these conditions the following were observed (see Fig. 1).

- External intercostal nerve discharges showed a biphasic pattern of discharges, with an expiratory burst in addition to the inspiratory one (cf. Tian & Duffin, 1996).
- EMG recordings from the most proximal region of the internal intercostal muscle showed a predominantly inspiratory pattern, as did recordings from the internal intercostal nerve branch that innervates it, though when expiration was strong the pattern was biphasic. Denervation of neighbouring intercostal spaces, plus destruction of the external intercostal layer and of multiple levator costae muscles (inspiratory) confirmed that the EMG activity arose from the sampled area. Some motor units were active in both the expiratory and the inspiratory bursts.
- Intracellular recordings included 2/3 external intercostal nerve motoneurones with expiratory depolarizations and 19/56 internal intercostal nerve motoneurones with biphasic depolarizations. The biphasic patterns often appeared to include simultaneous excitation and inhibition during inspiration.

The spatial distribution of these patterns and their functional significance have yet to be explored.

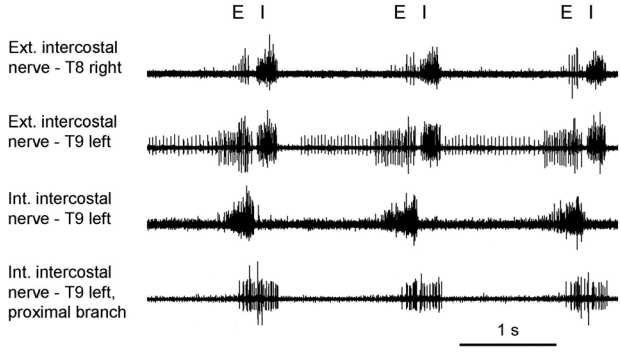

Figure 1. E, expiration; I, inspiration (chloralose).

De Troyer A et al. (2005) Physiol Rev 85, 717-756.

We have now confirmed at protein level, in addition to mRNA level, an increase in expression of NPY Y_1, and Y_2 receptors in diabetic rat tail arteries, which may explain their increased contribution to vasoconstriction seen previously (Kerlin *et al*., 2006). Our on-going studies have shown that NPY Y_5 receptors are not involved in vasoconstriction in control or diabetic tissues, although NPY Y_5 mRNA is down-regulated in diabetes. Therefore, of these changes, only the increase in NPY Y_1 and NPY Y_2 expression are of consequence for contraction.

Chow WL *et al*., (2001). Br J Pharm 134, 179-187.

Kerlin E, *et al*., (2006). Proc Physiol Soc 3, C62.

Tesfamariam B & Cohen CA (1995). Cardiovasc Res 29, 549-554.

We thank the School of Medicine, QUB, for their support (PD).

Where applicable, the authors confirm that the experiments described here conform with The Physiological Society ethical requirements.

C14 and PC63

A repressor of neuronal genes inhibits cardiac hypertrophy

L. Ooi, A. Bingham and I.C. Wood

Institute of Membrane and Systems Biology, University of Leeds, Leeds, UK

The most common disorder causing sudden cardiac death in young people is the cardiac disease, hypertrophic cardiomyopathy (HCM). Recent studies have suggested that HCM is more common than previously reported and it is now estimated that approximately l in every 500 people in the UK suffer from the disease. HCM is characterised by cardiac hypertrophy, an abnormal thickening of the heart muscle and while most affected individuals show few or no symptoms, others suffer heart failure, arrhythmias, and sudden death. The reason for the emergence of these symptoms in some people, but not others, remains unknown but since the transcriptional levels of a number of genes are indicative of the disease phenotype, the control of transcriptional programs could provide one mechanism to alleviate HCM.

The genes encoding the brain and atrial natriuretic peptides (BNP and ANP) are normally highly expressed in the foetal heart with levels reducing during development. High levels of expression of these genes are observed in adult ventricular myocytes in cardiac hypertrophy. One transcription factor that is important in repressing ANP and BNP expression in the normal adult heart is the Repressor Element 1-Silencing Transcription factor (REST). The aim of this study was to investigate the molecular mechanisms of REST-mediated repression and its potential role in hypertrophy. This was achieved by interrogating protein-DNA interactions and chromatin modifications at REST binding sites by chromatin immunoprecipitation and RT-PCR. REST represses its target genes by recruiting two distinct corepressor complexes that include histone deacetylases (HDAC1, HDAC2) and a H3 lysine 4-specific demethylase (LSD1). Inhibition of REST function resulted in an increase in ANP and BNP gene expression that correlated with increases in histone acetylation and dimethylation of H3 lysine 4 at the ANP and BNP promoters. Additionally, increasing REST expression in adult rat cardiomyocytes prevented increases in ANP and BNP expression by the hypertrophic agonist, endothelin-1. This data provides evidence that a therapeutic strategy aimed at augmenting REST and/or the action of its corepressors may be effective in treating cardiac hypertrophy.

This work was supported by the British Heart Foundation.

Where applicable, the authors confirm that the experiments described here conform with The Physiological Society ethical requirements.

C15 and PC64

Two mechanisms mediate the noradrenergic slow depolarization in rat tail artery

N. Rummery and J.A. Brock

Prince of Wales Medical Reseach Institute, Sydney, NSW, Australia

In rat tail artery, electrical stimulation of the sympathetic nerves evokes both an ATP-mediated excitatory junction potential (EJP) and a slower noradrenaline-mediated depolarization (NAD). Here we investigated the mechanisms underlying the NAD. Segments of proximal tail artery isolated from rats were mounted in a 1 ml recording chamber and the perivascular axons were electrically stimulated via a suction electrode applied to the proximal end. Intracellular recordings were made from the vascular smooth muscle cells. Application of the α_1-adrenceptor antagonist prazosin (0.1 μM, n = 6) slowed the rising phase of the NAD but did not change its amplitude or duration. In contrast, the α_2-adrenoceptor antagonist idazoxan (1 μM, n = 6) did not change the onset of the NAD but it did reduce its amplitude and duration. The combined application of prazosin and idazoxan abolished the NAD. In the presence of prazosin, the NAD was completely blocked by the K_{ATP} channel blockers, glybenclamide (10 μM, n = 6) and PNU 37883A (5 μM, n = 6). These agents also produced membrane depolarization. The NAD remaining when α_2-adrenoceptors were blocked was not affected by glybenclamide (10 μM, n = 5). In rat tail artery, the time constant of decay of the EJP is determined by the membrane time constant (Cassell *et al.*, 1988). The time constant of decay of EJPs evoked at the peak of the idazoxan-resistant NAD was prolonged (relative change 1.16 ± 0.03, $P < 0.01$, n = 6) suggesting that the α_1-component of the depolarization is also mediated by closure of K^+ channels. However, this component was not inhibited by broad-spectrum K^+ channel blockers (tetraethylammonium, 4-aminopyridine, Ba^{2+}). The idazoxan-resistant NAD was also unaffected by the Cl^- channel blockers, 9-anthracene carboxylic acid (100 μM, n = 4) and niflumic acid (10 μM, n = 3). These findings indicate that the NAD has two components; one which is due to activation of α_1-adrenoceptors and the other to activation of α_2-adrenoceptors. The α_2-adrenoceptor-mediated component is due to closure of K_{ATP} channels whereas α_1-adrenoceptor mediated component is most likely mediated by closure of another type of K^+ channel.

Cassell JF *et al.* (1988). *J Physiol* **397**, 31–49.

Where applicable, the authors confirm that the experiments described here conform with The Physiological Society ethical requirements.

C16 and PC65

Location and stretch-induced translocation of mechanotransductive proteins to and from caveolae in the adult heart

S. Calaghan and E. White

Institute of Membrane and Systems Biology, University of Leeds, Leeds, UK

Stretch activates an array of signalling pathways in the heart, regulating the force and rhythm of contraction and gene expression. A role for caveolae, invaginated lipid rafts lined with caveolin, in sensing and transducing mechanical stimuli has been proposed, but direct evidence for this is lacking in the adult cardiac myocyte. Here we investigate the caveolar localisation of 3 proteins linked with the contractile (eNOS, NHE) and electrical (TREK1) response of the heart to stretch, and determine the time-dependent effect of stretch on the distribution of caveolin 3 (Cav3), eNOS, NHE and TREK1.

Left ventricular (LV) pressure (measured via a balloon in the LV attached to a pressure transducer) and LV monophasic action potentials (MAPs) were recorded in Langendorff-perfused adult rat hearts. Some hearts were stretched by inflating the balloon to give 95% of maximum developed pressure; inflation was maintained for 10 or 30 min. To obtain caveolae-enriched membranes, LVs were fractionated on a discontinuous sucrose gradient following detergent-free Na_2CO_3 extraction.

Stretch caused both an immediate and a secondary slow increase in developed pressure (P<0.05 vs. pre-stretch or immediately post-stretch respectively; paired Student's t-test; n=14 hearts). MAP duration at 75% and 90% repolarisation was prolonged immediately after stretch (P<0.05). Buoyant caveolae-containing fractions (BF; 4-6 of 12) were enriched in Cav3 but excluded the non-caveolar marker β-adaptin, which was found predominantly in heavy fractions (HF; 9-12). In the absence of stretch, 100% of eNOS and NHE1 was found in BFs, whereas 96 ± 4% of TREK-1 was outside BFs (mean ± S.E.M; n=7). Stretch caused a translocation of Cav 3 from caveolae; at 30 min after stretch the ratio of Cav 3 in BF/HF was reduced from 1.6 ± 0.2 to 1.1 ± 0.1 (P<0.05, t-test; n=7). For the mechanotransductive proteins, the relationship between % in BF and time of stretch showed a tendency for eNOS (R=-0.93) to move from caveolae and for TREK1 (R=+0.91) to move to caveolae. NHE1 distribution did not change with stretch (R=-0.11).

In conclusion, some proteins (eNOS, NHE) involved in mechanotransduction in the adult heart are located exclusively in caveolae. Our data illustrate the dynamic nature of caveolae in response to mechanical stimuli. Stretch causes progressive movement of Cav3 from caveolae, consistent with disruption of caveolar structure, and translocation of eNOS from, and TREK1 to, caveolae. Because caveolae can modify signalling by concentrating or excluding elements of signal transduction cascades, and because Cav3 itself can interact to regulate protein activity, translocation of proteins to/from caveolae lends weight to the hypothesis that these microdomains are involved in mechanotransduction in the heart.

Sponsored by the British Heart Foundation.

Where applicable, the authors confirm that the experiments described here conform with The Physiological Society ethical requirements.

PC1

Amplified respiratory-sympathetic coupling in neonatal and juvenile spontaneously hypertensive rats

A. Simms[1], J.F.R. Paton[2], A.M. Allen[1] and A.E. Pickering[3]

[1]Department of Physiology, University of Melbourne, Melbourne, VIC, Australia, [2]Physiology and Pharmacology, University of Bristol, Bristol, UK and [3]Anaesthesia, University of Bristol, Bristol, UK

Sympathetic nerve activity (SNA) is elevated in mature spontaneously hypertensive (SH) rats compared to their normotensive Wistar-Kyoto (WKY) controls [1, 2]. However, it is unclear whether altered sympathetic activity is a cause or a consequence of hypertension. We tested the hypothesis that sympathetic nerve activity is elevated in pre-hypertensive neonate and juvenile SH rats, and that this may be due to augmented respiratory-sympathetic coupling. Using the working heart brainstem preparation [3], perfusion pressure, phrenic nerve and thoracic (T8) SNA were recorded in male SH and WKY rats at three ages; neonates (postnatal day 9-14), 3-week-old and 5-week-old (n=30). At comparable perfusion flow rates, pressures were higher in SH rats at all ages. Although the mean level of SNA was only higher in neonatal SH rats the amplitude of respiratory-related bursts of SNA were significantly greater in SH rats of all age groups (p<0.05). This was reflected in significantly larger respiratory-related oscillations in perfusion pressure (so called Traube-Hering waves) in SH than WKY rats at all ages (neonates 0.6±0.4 vs. 1.8±0.4mmHg; 3-week-old 2.8±0.7 vs. 5.6±1.5mmHg; 5-week-old 1.5±0.8 vs. 9.8±1.5mmHg, WKY v SHR respectively; Students t test, n=5/group, p<0.05). We assessed the respiratory-sympathetic coupling using phrenic-triggered averaging of the integrated sympathetic nerve recordings across 20 phrenic cycles. This revealed a shift in the peak of respiratory-sympathetic coupling from the post-inspiratory to the inspiratory period with increasing age in SH rats. Thus, increased SNA is already present in SH rats in early postnatal life and they show augmented respiratory modulation at all ages. This is reflected in altered vascular function, even in the "pre-hypertensive" phase, with elevated perfusion pressure and increased magnitude of Traube-Hering waves. We speculate that the amplified respiratory-related bursts of SNA seen in the neonate and juvenile SH rat may be a causal factor in the development of neurogenic hypertension in adulthood.

Judy WV & Farrell SK (1979). Hypertension 1(6), 605-614.

Schlaich MP et al. (2004). Hypertension 43(2), 169-175.

Paton JFR (1996). J Neurosci Methods 65(1), 63-68.

This work was funded by the BHF and NHMRC.